IEEE Access
Multidisciplinary ⋮ Rapid Review ⋮ Open Access Journal

Received January 17, 2019, accepted January 30, 2019, date of publication February 4, 2019, date of current version February 22, 2019.

Digital Object Identifier 10.1109/ACCESS.2019.2897219

Automotive Antenna Roof for Cooperative Connected Driving

GERALD ARTNER[1], (Member, IEEE), WIM KOTTERMAN[2], GIOVANNI DEL GALDO[2,3], (Member, IEEE), AND MATTHIAS A. HEIN[2], (Senior Member, IEEE)

[1]Institute of Telecommunications, Technische Universität Wien, 1040 Vienna, Austria
[2]Thuringian Centre of Innovation in Mobility, Technische Universität Ilmenau, 98693 Ilmenau, Germany
[3]Fraunhofer Institute for Integrated Circuits IIS, 91058 Erlangen, Germany

Corresponding author: Gerald Artner (gerald.artner@nt.tuwien.ac.at)

This work was supported in part by TU Ilmenau, in part by TU Wien, and in part by the TU Wien University Library through its Open Access Funding Program.

ABSTRACT An automotive concept for vehicular communications is proposed that utilizes the potential of the roof area for antennas. Antennas are distributed in cavities and on shelves in the center and on the front and rear roof ends. The arrangement of antennas on the roof allows better radiation to the front and back of automobiles than shark-fins and single cavities. Combining several modules provides space for further antennas, sensors, and integrated front-ends, as well as better spatial separation for multiple-input multiple-output (MIMO) arrays beyond 5G, and cooperative connected and automated driving. A prototype was developed and built into a car chassis. The measured data were analyzed and evaluated in the view of coverage for vulnerable road users and on correlation for the MIMO.

INDEX TERMS Antenna, automotive, concealed, conformal, chassis module, roof.

I. INTRODUCTION

Cooperative, connected and automated driving and communications beyond 5G will further increase the demand for vehicular antennas. There is a gap between the antenna systems that are required for automated and connected "self-driving" cars and the modules that are used today. Contemporary automotive antennas are placed in protruding aerodynamic casings which are about the same size as smart phones and do not fully utilize the available space on cars. Starting with a single antenna for telephony [1], the number of antennas included in these shark-fins has grown substantially during the last ten years. These modules now contain antennas for satellite navigation, multiple-input multiple-output (MIMO) antennas for cellular systems, WLAN, digital audio broadcasting, satellite digital audio radio (SDARS), and diversity antennas for vehicle-to-any communication (V2X) [2]–[9]. However, the antenna design suffers from the limited space: The coupling between antennas is significant and the antennas shadow each others radiation patterns. Several investigations conclude that automotive antenna systems benefit from spatial diversity, i.e. placing antennas further apart. MIMO channel measurements suggest that spatial diversity is more relevant than polarization diversity on vehicles [10]. Drive tests compared two antennas in a shark-fin module to antennas on the left- and right-hand side of the roof and it is found that the farther spaced antennas achieve a 15 % higher throughput [11].

Protruding modules cannot grow in size as they influence the vehicle aerodynamics and disturb their aesthetic appearance, which is a major selling point for passenger cars. Concepts of antennas not visible at first glance and conformal with the car body are now widely considered as alternative to shark-fin modules. Conformal modules can grow in size as they are not constrained by aesthetics. On the front end of the roof, modules at the rear view mirror are considered [12], spoilers are considered at the rear roof end [13], [14], transparent antennas can be applied to the windows [15], [16] and characteristic mode analysis can be utilized to excite parts of the vehicle [12], [17]. Side mirrors are a viable option for trucks [18], but may get replaced by camera systems. Overall, none of these positions are large enough to contain all antennas required in the future. Additionally, most are interdependent with other functional car units.

Optimum positions for automotive antennas are difficult to identify. Antenna characteristics change in a non-trivial way when placed on vehicles, due to a multitude of near-field effects that modify the intended current distributions [19].

The associate editor coordinating the review of this manuscript and approving it for publication was Di Zhang.

Common effects include diffraction, reflection, surface waves, re-radiation from induced currents and shadowing. Nevertheless, several studies compared antenna positions on cars [20], [21]. Reference [20] investigated performance based on data rates achieved in ray tracing simulations and identified the side mirrors, roof, A-pillars and the area above the windshield as promising positions.

For these reasons, integrating the antennas into the vehicle roof is a promising paradigm. Roofs contain overhead consoles or windows, but leave plenty of space otherwise. Due to its predominantly metallic structure, the roof acts as a large ground plane and it offers unobstructed omnidirectional radiation and isolation from the passenger cabin. An aperture towards the cabin has been considered in [22]. A carbon fiber reinforced cavity was described in [23] that can be manufactured as part of the chassis. Reference [24] showed that near-omnidirectional radiation is achievable from such a cavity with a variety of antennas. For single omnidirectional antennas circular cavities have been proposed [25]–[28]. Reflections from the side walls were prevented by either exponentially tapering the cavity floor [25], or by tilting the walls [24], [26]. Cavity-backed antennas have been proposed for automotive applications in [27] and [28]. Conformal antenna modules at the front of the roof [29], [30] were shown to increase coverage towards vulnerable road users [31] and they leave room to include optical cameras for automated driving cars. Pattern reconfigurable antennas in a chassis antenna cavity were prototyped in [32] and [33]. Smaller versions of such cavities have been used to flush-mount antennas on racing cars [34].

Contribution — We propose to turn car roofs into distributed antenna systems. Three antenna modules are combined in the car roof (Fig. 1a). The first is a cavity above the windshield, which is open towards driving direction. The second is a cavity in the roof center. The third is a shelf at the rear end of the car roof. The antenna roof was prototyped on a sedan type car mock-up and measured. The antennas are evaluated based on matching, coupling, correlation, gain patterns and their coverage towards vulnerable road users.

II. ANTENNA MODULES AND EVALUATION

We prototyped an automotive antenna roof concept that included three antenna modules at the front, center and rear of the roof (Fig. 1b). The modules in the front and center positions were conformal antenna cavities, while a shelf was tested at the rear roof end. The combination of three modules created more space for antennas on cars. The modules were spaced as far apart as possible on a car roof to achieve better separation of the antennas and to beneficially utilize the roof curvature, without compromising stability. The two cavities and the shelf were laser cut and bent from aluminum sheets. The paint was grinded off around the modules, then gaps were closed with conductive and adhesive aluminum tape. We expect that such antenna modules will have manufacturing costs similar to shark-fin modules in mass production. Like shark-fin modules, they will have a metal base, the antennas,

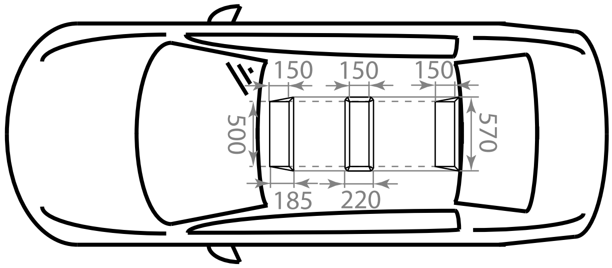

(a)

(b)

FIGURE 1. a) Sketch of the proposed antenna roof. b) Photograph of the antenna roof prototype on a sedan type passenger car mock-up. Antenna modules are located at the front, center and rear of the roof. All dimensions are in millimeter.

matching circuits, transceiver electronics and a dielectric cover.

A. CAVITY AT FRONT ROOF END ABOVE WINDSHIELD

The first antenna module was built at the front end of the car roof. A regular chassis antenna cavity with four walls at this position was considered in simulations in [35]. Instead of this straightforward approach, the investigated antenna module used the roof curvature as an advantage. The front wall obstructed the antenna in driving direction and was removed. The cavity is identical to the one in [31] and has a base plate size of 150 mm $\times$500 mm. The roof was cut open behind the A-pillar roof frame cross member in a distance of 13 cm from the windshield. The module was inserted into the car roof horizontally and the side walls were adapted to follow the roof curvature. Fig. 2a shows a closeup of the front antenna module.

B. CHASSIS CAVITY IN ROOF CENTER

The antenna module in the roof center was a chassis antenna cavity. The geometry of the aluminum cavity was identical to [24] to maintain comparability with previous work. The non-resonant cavity had tilted walls and a size of 150 mm $\times$ 500 mm on the floor and 220 mm $\times$ 570 mm at roof level. It was inserted into the roof behind the B-pillar roof frame cross member. The aluminum cavity is shown in Fig. 2b. Multiple antennas inside such a cavity are investigated in [36], where influence on the gain patterns is

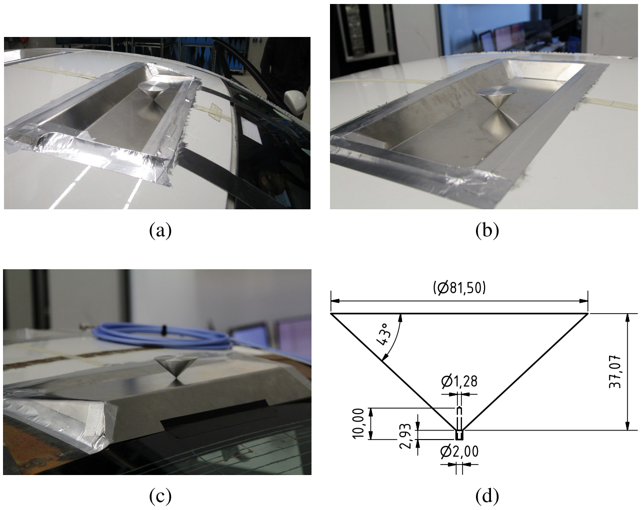

FIGURE 2. a) Antenna module on the front roof end above the windshield. b) Chassis antenna cavity in the roof center. c) Antenna shelf at the rear roof end. d) Cross section of the wideband conical monopole antenna. (Drawing reused with permission from [31], ©2018 IEEE.) All dimensions are in millimeters.

found due to the proximity of the antennas inside a single cavity.

C. SHELF AT REAR ROOF END ABOVE REAR WINDOW

The rear end of the car roof is more flexible with regard to antenna design and several options are available. Shark-fins, roof spoilers or cavities open towards the back of the car could be implemented. Instead of using an additional cavity, an antenna shelf concept was explored at the rear end. The shelf placed the antenna at an elevated position to allow unobstructed coverage around the car. Electronic circuits placed under the shelf would be isolated towards both antennas and the passenger cabin. Additionally, this position could act as a connecting point towards on-glass antennas in the rear window [17]. The dimensions were the same as the cavities (150 mm ×500 mm), but the side plates were bent downwards to form a shelf. The shelf was placed on the roof on top of the C-pillar roof frame cross member. The module back ended directly at the roof end, where the rear window glass started. The prototype is shown in Fig. 2c.

D. EVALUATION

First, the scattering parameters are evaluated to check proper matching of the antennas to the cable impedances and to quantify coupling between the antennas.

Second, the positions are evaluated based on gain patterns. Automotive antennas should provide omnidirectional coverage around the vehicle, as the orientation of the car towards other stations is generally unknown. Good coverage below horizon is paramount to communicate with vulnerable road users in the cooperative driving paradigm, and it is important for communication with smaller vehicles.

Third, the antenna modules are evaluated for their coverage towards vulnerable road users in front of the car. In [37] the position of cyclists and pedestrians three seconds before impact are quantified. It is found that 90 % of pedestrians are located within ±20° before impact, and that cyclists come from a wider range with 90 % within ±80°. These numbers allow a meaningful quantitative comparison of automotive antennas. Gain patterns in the horizontal plane ($\theta = 90°$, roof level) are considered for communication with vulnerable road users, on the basis that wearable antennas might be located at approximately roof level, i.e. 1.5 m above street level [38], [39].

Finally, the antenna system is evaluated for application in MIMO schemes by the correlation. The complex correlation is calculated from S-parameters by the expression [40]

$$\rho_{ij} = \frac{-\left(S_{ii}^{*}S_{ij} + S_{ji}^{*}S_{jj}\right)}{\sqrt{\left(1 - |S_{ii}|^2 - |S_{ji}|^2\right)\left(1 - |S_{jj}|^2 - |S_{ij}|^2\right)}} \tag{1}$$

where * denotes the conjugate complex. Eq. 1 is only valid for lossless antennas. This assumption should be approximately valid, because the conical monopole antennas and the roof around them are made from metal and no lossy substrate is used. The frequency dependent correlation is calculated from the measured S-parameters by evaluating Eq. 1 at each frequency point independently. Power correlation is then calculated as the magnitude square of the complex correlation.

III. MEASUREMENT SETUP AND RESULTS

All measurements were performed with a mid-sized passenger car mock-up in the Virtual Road Simulation and Test Area (VISTA) at the Thuringian Centre of Innovation in Mobility at TU Ilmenau, Germany [41]. VISTA employs a spherical near-field measurement system. Elevation angles from zenith to 20 degrees below horizon were covered with 110 probe antennas on the θ-arm. The setup is shown in Fig. 3. Far-field results were obtained by a near-to-far-field transformation. Antenna gain was calibrated using a reference monocone antenna.

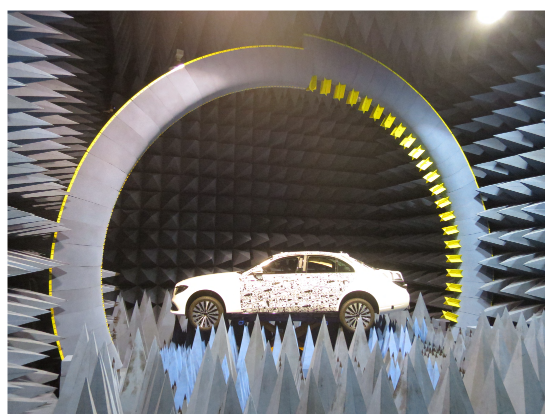

FIGURE 3. The prototype of the roof distributed antennas on the mock-up is set up in the VISTA for measurements [41].

Specifically designed narrow-band and multi-band antennas will be used for commercial systems. However, in order to evaluate the antenna positions and modules it is desired to measure standard wideband antennas. For this purpose, conical monopole antennas [42], [43] were used to characterize the antenna positions in a wide frequency range from 0.8 to 6 GHz. The cone angles were adapted to match the antenna impedances to the 50 Ohm feed cable impedances. Identical cones were turned on a lathe from aluminum. Holes were laser-cut in the center of each antenna module and coaxial SMA connector flanges were attached. The cones were not soldered to the connectors. Instead the cones were built with a cylindrical extension with a hole at the cone tip. The extension was designed to tightly fit to the inner conductors of the SMA connectors. The constructional drawing with dimensions is given in Fig. 2d. During measurements all three antenna modules were present on the vehicle. Not-measured antennas present during the gain pattern measurements were terminated with matched loads. Protective covers were not used, such that the results do not depend on an arbitrarily chosen radome.

The scattering parameters were measured in an anechoic environment and are given in Fig. 4. The return loss of the conical monopole antennas is better than 10 dB over most of the frequency band and is slightly influenced by the mounting position. The decoupling between the antennas is excellent, which is achieved by the large distances between the antennas on the roof. It is slightly above −30 dB for neighboring antennas and frequencies around 1 GHz (maximum −28 dB for front-to-center and −26 dB for center-to-rear), e.g. the lower LTE bands. For higher frequencies decoupling approaches −40 dB. The antennas in the front cavity and on the rear shelf are even better decoupled with a worst case value of −35 dB throughout the measured frequency range from 0.85 to 6 GHz. Such values are practically unachievable in shark-fin modules, because of the close proximity of the antennas and the resulting coupling of the fields. For comparison, the two monopole-like antennas used in [6], reached a mutual coupling of −6 dB below 1 GHz and −15 dB around 6 GHz. [5] achieved −10 dB around 1 GHz, −20 dB to −30 dB at 2.4 GHz and −30 dB at 5.9 GHz, in a shark-fin module where PIFA and monopole antennas were combined. A combination of PIFA and stacked monopole in [7] achieved −10 dB on the 800 MHz bands and −20 dB above this band.

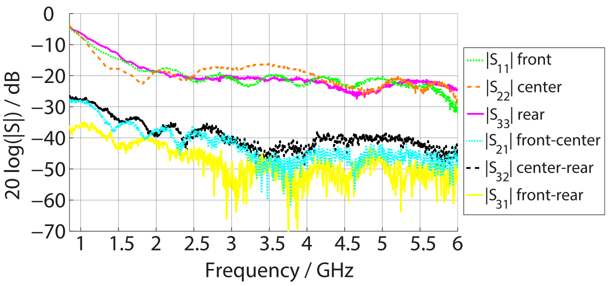

FIGURE 4. **Absolute values of the measured scattering parameters. $|S_{11}|$, $|S_{22}|$, $|S_{33}|$ quantify the matching of the antennas in the front, center and rear roof locations, respectively. $|S_{21}|$, $|S_{32}|$, $|S_{31}|$ quantify the coupling between antennas in front/center, center/rear and front/rear locations, respectively.**

Cuts of the measured gain patterns are shown in Fig. 5. The vertical cuts in front and back direction show that the cavity at the front is more efficient in the front direction (Fig. 5a), while the roof shelf at the rear end offers better coverage towards the back (Fig. 5c) and the chassis cavity in the roof center is a good tradeoff (Fig. 5b). The antenna positions have similar characteristics towards the sides of the car (Figs. 5d-5f). This is no surprise, because from the viewpoint of each antenna the geometry is similar towards the sides. The gain patterns for 2.45 GHz and below are typical monopole patterns with a null at zenith and smooth omnidirectional coverage towards horizon. For 5.9 GHz large ripples appear close to zenith. Gain is reduced by about 10 dB from 30° to 60° and deep nulls appear in this region. This is a direct influence of the chassis antenna cavity design and was already found in [24]. For $\theta > 60°$ the gain pattern is again omnidirectional, which is important for the V2X application at 5.9 GHz.

In the horizontal plane all three antenna modules offer omnidirectional coverage around the whole vehicle, with gains >−10 dBi. No nulls appear in the gain patterns at the horizon, in contrast to the typical performance of closely spaced antennas in shark-fins and roof spoilers [5]–[7], [13], [14].

The coverage towards vulnerable road users is compared in Tab. 1 and Tab. 2, where the minimum, maximum and average gains of the three antenna modules are given for pedestrians and cyclists, respectively. As expected, the cavity above the windshield provides the best coverage towards vulnerable road users. Interestingly, the antenna on the rear shelf surpasses the center cavity for some of the selected frequencies. This is a direct consequence of the elevated antenna position on the shelf and the resulting improvement in coverage towards the front. It must however be noted that the coverage from the center cavity and rear shelf decay abruptly in the front towards angles below horizon (compare Figs. 5a, 5b and 5c), just as it is the case for contemporary shark-fin modules. If pedestrians carry devices in their pant pockets or handbags [44], then coverage from the center and rear roof end might be significantly decreased, which is why the module at the front is so important.

Results for correlation are shown in Fig. 6 for all antenna pairs. Note that the correlation is logarithmically scaled, although the correlation is usually depicted linearly for closely spaced MIMO antennas, e.g. [40]. Modules placed next to each other (front-center and center-rear) are spaced by at least 62 cm – even at the lower LTE frequency bands this is almost 2 λ. The low coupling between the antennas ($|S21|_{max} = -28$ dB and $|S21|_{max} = -26$ dB) causes maximum correlations of $|\rho_{12}|^2_{max} = 0.0029$ and $|\rho_{23}|^2_{max} = 0.0045$ at 850 MHz. The antennas in the front and rear end are separated by 124 cm (3.5 λ at 850 MHz), which results in $|\rho_{13}|^2_{max} = 3 \cdot 10^{-5}$. As comparison, [8] investigated two dielectric resonator antennas inside a

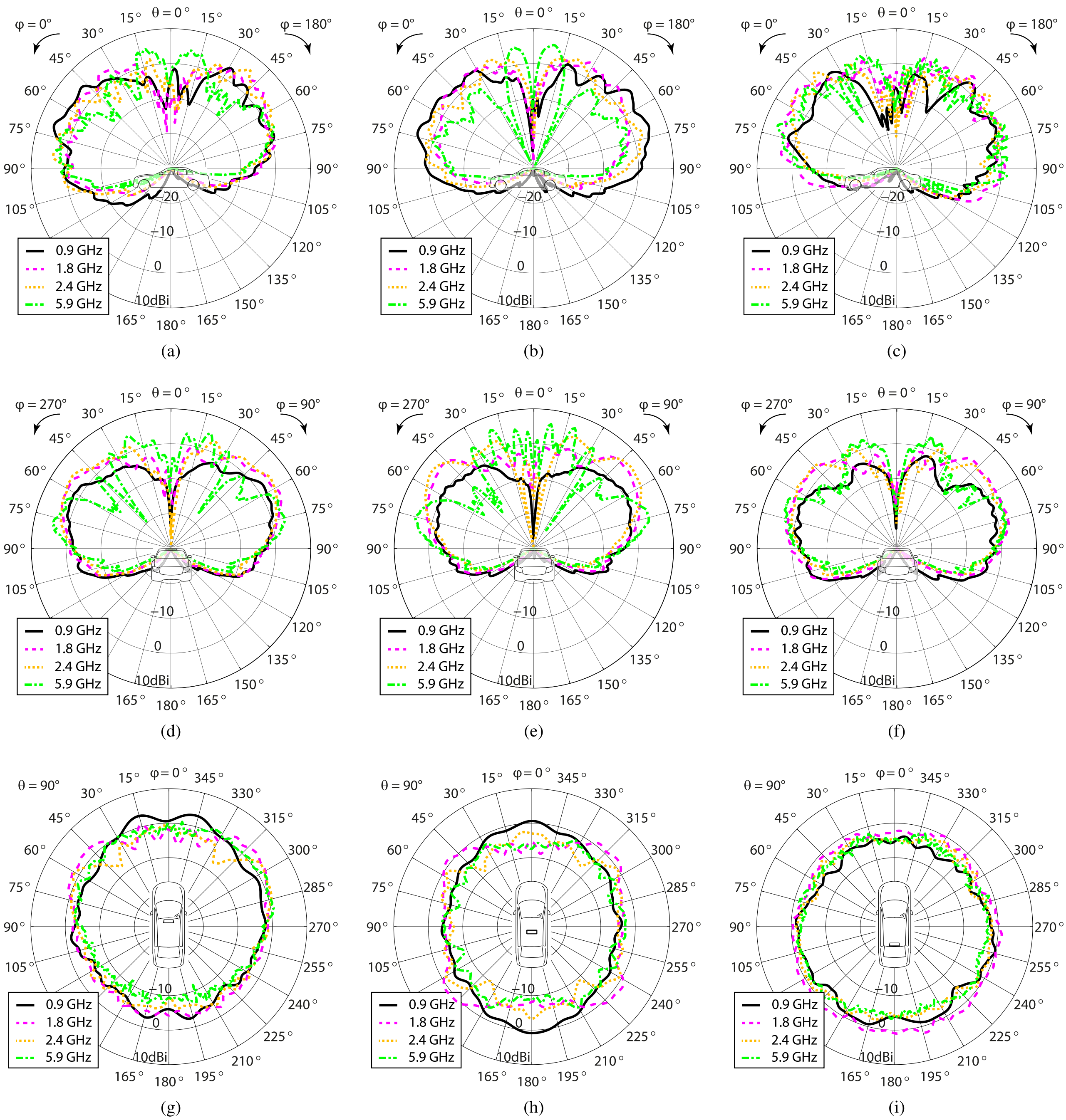

FIGURE 5. Cuts of the gain patterns measured in situ on a sedan mock-up; realized gain; linear polarization in θ direction; top-row (a, b, c): vertical cuts front/back, middle-row (d, e, f): vertical cuts left/right and bottom-row (g, h, i): horizontal cuts for polar angle $\theta = 90°$. Left-column (a, d, g): front cavity, middle-column (b, e, h): center cavity and right-column (c, f, i): rear shelf.

TABLE 1. Minimum, maximum and average gains towards pedestrian in dBi ($\theta = 90°$, $\varphi = \pm 20°$).

	front cavity			center cavity			rear shelf		
frequency	min	max	mean	min	max	mean	min	max	mean
0.9 GHz	0.49	3.18	2.14	-1.87	0.62	-0.66	-6.29	-3.74	-4.93
1.8 GHz	-6.16	0.51	-2.93	-8.73	-5.08	-6.58	-3.27	-1.25	-2.54
2.4 GHz	-3.00	-0.78	-2.09	-5.23	-2.47	-3.93	-5.54	-3.17	-4.47
5.9 GHz	-3.62	0.60	-1.56	-7.55	-4.79	-6.19	-6.00	-1.72	-4.19

shark-fin and achieved an envelope correlation of 0.2 in the 800 MHz LTE band and correlations <0.05 in the 1800, 2100 and 2600 MHz frequency bands. Schneider *et al.* [5] achieved a correlation between 0.1 and 0.2 in the 900 MHz band with two planar inverted-F antennas (PIFA) inside a shark-fin.

TABLE 2. Minimum, maximum and average gains towards cyclists in dBi ($\theta = 90°$, $\varphi = \pm 80°$).

	front cavity			center cavity			rear shelf		
frequency	min	max	mean	min	max	mean	min	max	mean
0.9 GHz	-3.83	3.18	-0.64	-5.86	0.62	-2.92	-6.98	-2.77	-4.95
1.8 GHz	-6.16	3.00	-0.47	-8.73	1.55	-2.91	-3.48	-0.14	-1.96
2.4 GHz	-7.89	2.04	-1.95	-8.89	-0.18	-4.02	-6.00	-1.28	-3.61
5.9 GHz	-3.62	1.58	-0.80	-8.03	-2.08	-5.04	-6.63	-1.29	-3.78

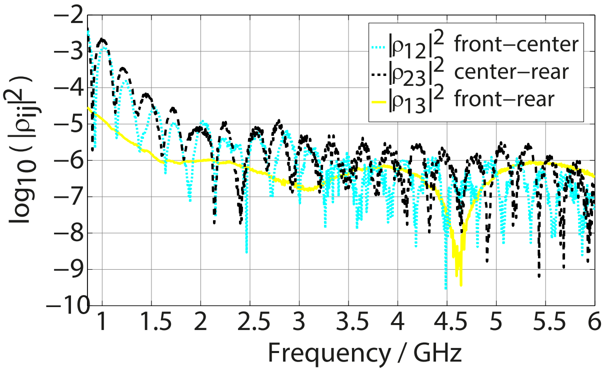

FIGURE 6. Antenna correlation calculated from measured S-parameters.

IV. CONCLUSION

An antenna concept is proposed which beneficially exploits the large size of cars by utilizing the full roof for antennas. Antennas are placed in two conformal cavities and on a shelf. The platforms are built into a non-functional pretest vehicle to show practical feasibility. The whole arrangement is measured inside an electromagnetically shielded anechoic chamber with a mid-sized passenger car mock-up.

The performance of the concept is evaluated based on matching, coupling, gain patterns, correlation and coverage towards vulnerable road users - all in a wide frequency range from 900 MHz to 6 GHz. The modules' influence on matching is small. The coupling of the antennas is extremely low due to their large separation, which is unachievable in state of the art shark-fin modules. Gain patterns are omnidirectional and no zeros are introduced in the horizontal plane, which is currently a major drawback in small modules where the antennas shadow each other. Coverage towards vulnerable road users is quantified based on user locations prior to accidents. A minimum gain above −9 dBi is achieved for all three positions and all investigated frequencies and the front cavity further increases this coverage. The correlation between the antennas is low, which is again a consequence of the distance between the antennas. MIMO transmission schemes can utilize the reduced correlation to increase throughput and antenna selection schemes can increase reliability for safety critical applications.

The performance achieved in this research motivates the application of significantly larger antenna constructs on vehicles. The conformal design brings beneficial side effects. The radomes are no longer visible and the vehicle aesthetics are improved, subject to taste. The antennas no longer protrude from the vehicle, which decreases the drag coefficient and in turn reduced fuel consumption and increases range per battery charge for electric vehicles.

ACKNOWLEDGMENT

This cooperation originated in the framework of COST Action CA15104 IRACON. The authors would like to thank T. Nowack, A. Weiß and F. Müller of TU Ilmenau, and R. Langwieser and H. Bauer of TU Wien for the measurements and mechanical modifications.

REFERENCES

[1] A. Walbeoff and R. J. Langley, "Multiband PCB antenna," *IEE Proc. Microw., Antennas Propag.*, vol. 152, no. 6, pp. 471–475, Dec. 2005.

[2] Q. Wu, Y. Zhou, and S. Guo, "An L-sleeve L-monopole antenna fitting a shark-fin module for vehicular LTE, WLAN, and car-to-car communications," *IEEE Trans. Veh. Technol.*, vol. 67, no. 8, pp. 7170–7180, Aug. 2018.

[3] A. Michel, P. Nepa, M. Gallo, I. Moro, A. P. Filisan, and D. Zamberlan, "Printed wideband antenna for LTE-band automotive applications," *IEEE Antennas Wireless Propag. Lett.*, vol. 16, no. 1, pp. 1245–1248, 2017.

[4] I. Goncharova and S. Lindenmeier, "Compact satellite antenna module for GPS, Galileo, GLONASS, BeiDou and SDARS in automotive application," *IET Microw., Antennas Propag.*, vol. 12, no. 4, pp. 445–451, 2018.

[5] O.-Y. Kwon, B.-S. Kim, and R. Song, "A fully integrated shark-fin antenna for MIMO-LTE, GPS, WLAN, and WAVE applications," *IEEE Antennas Wireless Propag. Lett.*, vol. 17, no. 4, pp. 600–603, Mar. 2018.

[6] D. V. Navarro-Méndez *et al.*, "Wideband double monopole for mobile, WLAN, and C2C services in vehicular applications," *IEEE Antennas Wireless Propag. Lett.*, vol. 16, pp. 16–19, 2017.

[7] N. Guan, H. Tayama, M. Ueyama, Y. Yoshijima, and H. Chiba, "A roof automobile module for LTE-MIMO antennas," in *Proc. IEEE-APS Top. Conf. Antennas Propag. Wireless Commun. (APWC)*, Sep. 2015, pp. 387–391.

[8] T.-L. Chiu, L. Huitema, O. Pajona, and T. Monediere, "Compact and multiband MIMO dielectric resonator antenna for automotive LTE communications," *Int. J. Antennas Propag.*, vol. 2018, Dec. 2018, Art. no. 8231081.

[9] C.-Y. Liou and S.-G. Mao, "Miniaturized shark-fin rooftop antenna with integrated DSRC communication module for connected vehicles," in *Proc. 32nd Gen. Assem. Sci. Symp. Int. Union Radio Sci. (URSI GASS)*, Aug. 2017, pp. 1–4.

[10] C. C. Squires and T. J. Willink, "The impact of vehicular antenna placement on polarization diversity," in *Proc. IEEE 70th Veh. Technol. Conf. Fall*, Sep. 2009, pp. 1–5.

[11] A. Thiel, L. Ekiz, O. Klemp, and M. Schultz, "Automotive grade MIMO antenna setup and performance evaluation for LTE-communications," in *Proc. Int. Workshop Antenna Technol. (iWAT)*, Mar. 2013, pp. 171–174.

[12] E. Safin, R. Valkonen, and D. Manteuffel, "Reconfigurable LTE MIMO automotive antenna system based on the characteristic mode analysis," in *Proc. 9th Eur. Conf. Antennas Propag. (EuCAP)*, Lisbon, Portugal, Apr. 2015, pp. 1–3.

[13] E. Condo Neira, J. Carlsson, K. Karlsson, and E. G. Ström, "Combined LTE and IEEE 802.11p antenna for vehicular applications," in *Proc. Eur. Conf. Antennas Propag. (EuCAP)*, Lisbon, Portugal, Apr. 2015, pp. 1–5.

[14] S. Hastürkoğlu and S. Lindenmeier, "A wideband automotive antenna for actual and future mobile communication 5G/LTE/WLAN with low profile," in *Proc. Eur. Conf. Antennas Propag. (EUCAP)*, Mar. 2017, pp. 602–605.

[15] J. H. Lee, S. H. Lee, D. Kim, and C. W. Jung, "Transparent antenna using a μ-metal mesh on the quarter glasses of an automotive for DMB service receiving," *Microw. Opt. Technol. Lett.*, vol. 60, no. 12, pp. 3009–3014, 2018.

[16] J. H. Lee, S. H. Lee, D. Kim, and C. W. Jung, "Transparent dual-band monopole antenna using a μ-metal mesh on the rear glass of an automobile for frequency modulation/digital media broadcasting service receiving," *Microw. Opt. Technol. Lett.*, vol. 61, no. 2, pp. 503–508, 2019.

[17] A. Asgharzadeh, J. Singh, P. Hofmann, G. Reichert, and M. A. Hein, "Design approach towards automotive FM broadcast antennas based on characteristic modes," in *Proc. IEEE-APS Topical Conf. Antennas Propag. Wireless Commun. (APWC)*, Sep. 2017, pp. 57–60.

[18] L. Marantis, D. Rongas, A. Paraskevopoulos, C. Oikonomopoulos-Zachos, and A. Kanatas, "Pattern reconfigurable ESPAR antenna for vehicle-to-vehicle communications," *IET Microw., Antennas Propag.*, vol. 12, no. 3, pp. 280–286, Feb. 2018.

[19] M. B. Diez, P. Plitt, W. Pascher, and S. Lindenmeier, "Antenna placement and wave propagation for Car-to-Car communication," in *Proc. Eur. Microw. Conf. (EuMA)*, Sep. 2015, pp. 207–210.

[20] T. Mahler, L. Reichardt, C. Heine, M. Pauli, and T. Zwick, "Channel based design of systems with multiple antennas," *Prog. Electromagn. Res. B*, vol. 64, pp. 63–81, 2015. [Online]. Available: http://www.jpier.org/PIERB/pier.php?paper=15090801

[21] M. E. Asghar, F. Wollenschläger, A. Asgharzadeh, J. Singh, and M. A. Hein, "Influence of antenna mounting location on the radiation pattern of an automotive antenna," in *Proc. 12th Eur. Conf. Antennas Propag. (EuCAP)*, 2018, pp. 1–5.

[22] L. Low, R. Langley, R. Breden, and P. Callaghan, "Hidden automotive antenna performance and simulation," *IEEE Trans. Antennas Propag.*, vol. 54, no. 12, pp. 3707–3712, Dec. 2006.

[23] G. Artner, "Carbon fiber reinforced polymer cavity for vehicular antennas," Ph.D. dissertation, Fakultät für Elektrotechnik Informationstechnik, Technische Universität Wien, Vienna, Austria, Dec. 2017.

[24] G. Artner, R. Langwieser, and C. F. Mecklenbräuker, "Concealed CFRP vehicle chassis antenna cavity," *IEEE Antennas Wireless Propag. Lett.*, vol. 16, pp. 1415–1418, 2017.

[25] S. Lee, G. Jeoung, and J. Choi, "Three-dimensional-printed tapered cavity-backed flush-mountable wideband antenna for UAV," *Microw. Opt. Technol. Lett.*, vol. 59, pp. 2975–2981, Dec. 2017.

[26] N. Nguyen-Trong, S. P. Pinapati, D. Hall, A. Piotrowski, and C. Fumeaux, "Ultralow-profile and flush-mounted monopolar antennas integrated into a metallic cavity," *IEEE Antennas Wireless Propag. Lett.*, vol. 17, no. 1, pp. 86–89, Jan. 2018.

[27] E. Gschwendtner and W. Wiesbeck, "Ultra-broadband car antennas for communications and navigation applications," *IEEE Trans. Antennas Propag.*, vol. 51, no. 8, pp. 2020–2027, Aug. 2003.

[28] J.-M. F. González, P. Padilla, J. F. Valenzuela-Valdés, J. L. Padilla, and M. Sierra-Castañer, "An embedded printed antenna with omnidirectional azimuth coverage for automotive applications," *IEEE Antennas Propag. Mag.*, vol. 60, no. 3, pp. 118–128, Jun. 2018.

[29] R. Weicker and M. Albo, "Vehicle window assembly and method for mounting a vehicle window assembly," U.S. Patent 9 126 469 B2, Sep. 8, 2015.

[30] L. L. Nagy, "Automobile roof antenna shelf," U.S. Patent 6 118 410, Sep. 12, 2000.

[31] G. Artner, W. Kotterman, G. Del Galdo, and M. A. Hein, "Conformal automotive roof-top antenna cavity with increased coverage to vulnerable road users," *IEEE Antennas Wireless Propag. Lett.*, vol. 17, no. 12, pp. 2399–2403, Dec. 2018.

[32] G. Artner, J. Kowalewski, C. F. Mecklenbräuker, and T. Zwick, "Automotive pattern reconfigurable antennas concealed in a chassis cavity," in *Proc. 20th Int. Symp. Wireless Pers. Multimedia Commun. (WPMC)*, Dec. 2017, pp. 265–270.

[33] G. Artner, J. Kowalewski, C. F. Mecklenbräuker, and T. Zwick, "Pattern reconfigurable antenna with four directions hidden in the vehicle roof," in *Proc. Int. Workshop Antenna Technol., Small Antennas, Innov. Struct., Appl. (iWAT)*, Mar. 2017, pp. 82–85.

[34] S. Zwickl-Bernhard, J. Steiner, A. Pöllinger, and G. Artner, "Carbon-fiber reinforced antenna cavity hidden in the monocoque of a racing car," in *Proc. IEEE 29th Annu. Int. Symp. Pers., Indoor Mobile Radio Commun. (PIMRC)*, Aug. 2018, pp. 1126–1127.

[35] I. M. Yousaf and B. K. Lau, "On performance of hidden car roof antennas," in *Proc. Eur. Conf. Antennas Propag. (EuCAP)*, 2018, pp. 1–5.

[36] G. Artner, "The communicative vehicle: Multiple antennas in a chassis antenna cavity," in *Proc. IEEE 86th Veh. Technol. Conf. (VTC)*, Sep. 2017, pp. 1–5.

[37] J. Lenard, R. Welsh, and R. Danton, "Time-to-collision analysis of pedestrian and pedal-cycle accidents for the development of autonomous emergency braking systems," *Accident Anal. Prevention*, vol. 115, pp. 128–136, Jun. 2018.

[38] S. J. Ambroziak *et al.*, "An off-body channel model for body area networks in indoor environments," *IEEE Trans. Antennas Propag.*, vol. 64, no. 6, pp. 4022–4035, Sep. 2016.

[39] M. G. Doone, S. L. Cotton, D. W. Matolak, C. Oestges, S. F. Heaney, and W. G. Scanlon, "Pedestrian-to-vehicle communications in an urban environment: Channel measurements and modeling," *IEEE Trans. Antennas Propag.*, to be published. doi: 10.1109/TAP.2018.2885461.

[40] X. Chen, P.-S. Kildal, and J. Carlsson, "Comparisons of different methods to determine correlation applied to multi-port UWB eleven antenna," in *Proc. 5th Eur. Conf. Antennas Propag. (EuCAP)*, Apr. 2011, pp. 1776–1780.

[41] M. A. Hein *et al.*, "Emulation of virtual radio environments for realistic end-to-end testing for intelligent traffic systems," in *Proc. IEEE MTT-S Int. Conf. Microw. Intell. Mobility (ICMIM)*, Apr. 2015, pp. 1–4.

[42] J. Ha, M. A. Elmansouri, and D. S. Filipovic, "A compact ultrawideband reflector antenna: Using a wide-band omnidirectional antenna with a mechanically steerable endfire beam to illuminate a half-cut paraboloid reflector," *IEEE Antennas Propag. Mag.*, vol. 60, no. 3, pp. 75–86, Jun. 2018.

[43] A. Heilmann, *Antennen, Band 1*. Mannheim, Germany: Bibliographisches Institut, 1970, pp. 108–111.

[44] F. Ichikawa, J. Chipchase, and R. Grignani, "Where's the phone? A study of mobile phone location in public spaces," in *Proc. 2nd Asia Pacific Conf. Mobile Technol., Appl. Syst.*, Nov. 2005, pp. 1–8.

GERALD ARTNER (M'13) was born in St. Pölten, Austria, in 1987. He received the degree in electronic engineering with a specialization in computer engineering from the secondary technical school in St. Pölten (HTL), in 2007, the B.Sc. degree in electrical engineering and information technology, the Dipl.Ing. (M.Sc.) degree in telecommunications, and the Dr.techn. (Ph.D.) degree in electrical engineering from the Technische Universität Wien, Vienna, Austria, in 2012, 2013, and 2017, respectively. He is currently a university assistant with the Institute of Telecommunications, Technische Universität Wien. His research interests include interference alignment, wireless communication testbeds, vehicular communications, automotive antennas, and carbon fiber reinforced polymer in antenna applications.

WIM KOTTERMAN graduated in physics from the Delft University of Technology, Delft, The Netherlands, in 1984. He received the Ph.D. degree in electrical engineering from Aalborg University, Aalborg, Denmark, in 2004. After a two-year stay at a small engineering and consulting firm in ultrasonics, he moved to Dr. Neher Labs, KPN, The Netherlands, as the former Incumbent Telecom and Mail Operator. In 2000, he moved to the Center for PersonKommunikation, Aalborg University. His thesis is on channel modeling for multi-antenna small handsets. Since 2004, he has been with Technische Universität Ilmenau, Ilmenau, Germany, where he has also been with the Institute of Information Technology, on various topics, ranging from channel measurements and modeling for wireless systems to over-the-air testing of wireless systems. In the last four years, he was associated with the Thuringian Centre of Innovation in Mobility, focusing on cooperative automated driving. His research interests include channel measurements, field strength prediction, and cell planning for the GSM networks.

GIOVANNI DEL GALDO (M'12) received the Dr.Ing. degree in telecommunications engineering from the Politecnico di Milano, Milano, Italy, and the Ph.D. degree in MIMO channel modeling for mobile communications from Technische Universität Ilmenau (TU Ilmenau), Ilmenau, Germany, in 2007. He then joined the Fraunhofer Institute for Integrated Circuits IIS, Erlangen, Germany, involved in audio watermarking and parametric representations of spatial sound. Since 2012, he has been leading a joint research group composed of a department with the Fraunhofer Institute for Integrated Circuits IIS and has also been a Full Professor and a Chair with TU Ilmenau in wireless distribution systems and digital broadcasting. His current research interests include the analysis, modeling, and manipulation of multidimensional signals, over-the air testing for terrestrial and satellite communication systems, and sparsity promoting reconstruction methods.

MATTHIAS A. HEIN (M'06–SM'06) received the Diploma and Ph.D. degrees (Hons.) from the University of Wuppertal, Wuppertal, Germany, in 1987 and 1992, respectively. He was involved in the exploration of super-conductor microwave applications in mobile and satellite communications. From 1998 to 2001, he headed an Interdisciplinary Research Group of passive microwave electronic devices. In 2002, he joined Technische Universität Ilmenau, Ilmenau, Germany, as the Head of the RF and Microwave Research Laboratory. His research interests include antenna and microwave engineering. He is an Elected Board Member of the IEEE Joint German Chapter MTT/AP and the European Association on Antennas and Propagation. He was the Chair of the German Microwave Conference, in 2012. He is the Designated Chair of the European Microwave Conference, in 2017. In 1999, he received a British Senior Research Fellowship of the Engineering and Physical Sciences Research Council, University of Birmingham, U.K. He served as a Co-Organizer and a Convener of various other international conferences. He acts as a referee for high-ranking scientific journals and funding agencies. In 2014, he became a Spokesman of the Thuringian Center of Innovation in Mobility, where his focus is on intelligent automotive wireless sensor and communication systems and virtual test drives.